Density functional theory (DFT) study on the interaction of ammonium (NH_4^+) and aromatic nitrogen heterocyclics

Wei-Liang Zhu,[ab] Hua-Liang Jiang,*[a] Chum Mok Puah,[b] Xiao-Jian Tan,[a] Kai-Xian Chen,[a] Yang Cao[c] and Ru-Yun Ji[a]

[a] *State Key Laboratory of Drug Research, Shanghai Institute of Materia Medica, Chinese Academy of Sciences, 294 Taiyuan Road, Shanghai 200031, P.R. China. E-mail: jiang@iris3.simm.ac.cn or jiang@mail.shcnc.ac.cn; Tel: +86-21-64311833, ext. 222; Fax: +86-21-64370269*

[b] *Department of Chemical Process & Biotechnology, Singapore Polytechnic, Singapore 139651*

[c] *Department of Chemistry, Suzhou University, Suzhou 215006, P.R. China*

Received (in Cambridge, UK) 1st April 1999, Accepted 1st September 1999

A DFT calculation was performed at the B3LYP/6-31G* level on the complexes formed by NH_4^+ and aromatic nitrogen heterocyclics, *viz*. pyrrole, imidazole, pyridine and indole, in order to investigate the mechanism and complexity of the interaction between the ammonium group and the aromatic heterocyclic in biomacromolecules. The optimized geometries suggested that there are two different types of complexes: one is a cation–π complex and the other is a hydrogen bond complex. A cation–π complex will be formed if the heteroatom has no localized lone-pair electrons. A hydrogen bond complex will be formed by proton transfer from NH_4^+ to the heteroatom if the heteroatom has localized lone-pair electrons. In the case of the cation–π complex, the predicted geometries, atomic charges and thermodynamic parameters revealed that ammonium binds more strongly to heterocyclics than it binds to benzene. The calculated orbital coefficient and the optimized structures implied that NH_4^+ interacts with the π electrons of the C=C bond of heterocyclics to form a cation–π complex mainly through one hydrogen atom. Regarding the hydrogen bond complex, although the calculated binding strength is similar to that for the cation–π complex, the ΔH of the whole reaction process suggested that the formation of the hydrogen bond complex is favorable to the stability of the whole system. Calculated IR spectra showed that three groups of new bands appear when NH_4^+ binds to heterocyclics. Normal mode analysis showed that these new bands are all related to the relative motion of the two parts in the formed complexes. All these results suggest that the NH_4^+–heterocyclic system is a better model for studying the nature and complexity of the interaction between the ammonium group and the aromatic ring structure in biomolecules.

Introduction

Increasingly it is becoming clear that cation–π interactions are implicated in a wide range of systems and should be considered as an important and general noncovalent binding force.[1] In order to reveal the nature of the cation–π interaction and investigate its role in life science, extensive experimental and theoretical efforts have been made in the past decade.[2–10] As a result, due to some available binding energies, cations have been shown to bind strongly to the π face of an aromatic system. Indeed this cation–π interaction may be stronger than hydrogen bond and hydrophobic interactions. For instance, a hydrophobic binding site comprised of aromatic rings can compete with full aqueous solvation in the binding of highly solvated cations.[11] These studies showed that a better understanding of the cation–π interaction might help us in designing new catalysts, drugs, proteins and enzymes as well as in developing a new molecular force field.[12]

Quantum chemistry calculations at a high level have provided an excellent complement to the experimental work. For instance, parameters that are difficult to obtain, *viz.* geometry and electron structures, of cation–π complexes have been obtained.[8–10,13–15] Because biomacromolecules are too big to be investigated using a high level theoretical method, smaller models that are indicative of the interactions present in biomolecules have been adopted in many investigations. Although benzene is the best π system model for sophisticated quantum chemistry calculations due to its high symmetry, it could not uncover the complexity of the aromatic ring in biomolecules. This is coupled with the fact that most of the π systems in biomacromolecules are nitrogen heterocyclics. Thus using the latter for investigation would be ideal. Amino groups are common in both biomolecules and substrates. Besides metal ions, the ammonium group can act as an important cation. To our knowledge, there is no systematic theoretical investigation on the interaction of ammonium cation and aromatic heterocyclics.[16]

DFT has recently been recognized as an efficient tool for studying molecular properties. It has additional advantages in that it can be used to treat bigger systems than can Hartree–Fock (HF) and Möller–Plesett (MP) methods; its computational resources are to N^3 while HF and MP are to N^4 to N^7. Our previous calculation results at the B3LYP[17]/6-31G, B3LYP/6-31G*, B3LYP/6-31G**, B3LYP/6-311++G**, MP2/6-31G* and MP2/6-31G** levels showed that the B3LYP/6-31G* method is good enough at least for calculating the thermodynamic properties and IR spectrum.[8–10,18–21] In addition, the enthalpy of formation, ΔH, free energy of formation, ΔG, and IR spectrum were perfectly in accordance with experimental results. Moreover, the basis set superposition errors (BSSEs) were found to be small in cation–π systems.[1,16] Therefore, the B3LYP/6-31G* method was used and BSSEs were not considered in this study.

The objectives of this study were (i) to determine the geometries and thermodynamic parameters of the complexes formed by NH_4^+ and heterocyclics; (ii) to find out the intrinsic

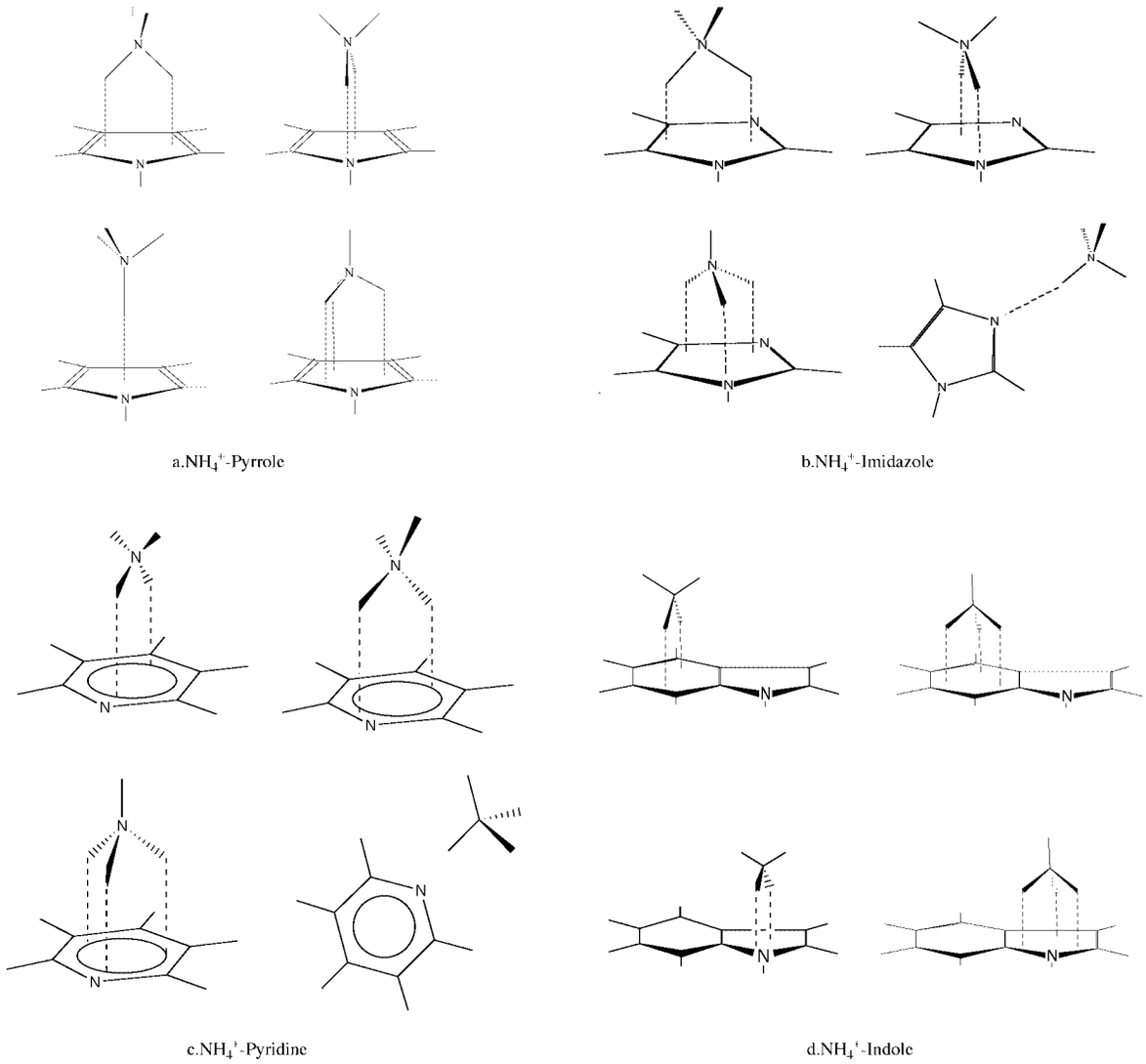

Fig. 1 Initial structures of the complexes of NH_4^+ and heterocyclics.

normal model of these complexes; and (iii) to gain further insight into the complexity of the interaction between the ammonium group and the heterocyclic structure in biomacromolecules. The cation selected in this study was NH_4^+, and the aromatic nitrogen heterocyclics were pyrrole, imidazole, pyridine and indole (Fig. 1). These represent complicated cationic ion and π systems in proteins and nucleic acids. Normally, it was found that there is no water molecule residing between the cation group and the aromatic ring in biomolecules,[22–24] implying that the binding interaction is a direct interaction. Hence, we did not take into consideration the role of the solvent in this study.

Computational details

Considering that the initial geometry might have crucial and pivotal influence on the final conformation of the cation–π complex, several possible initial geometries for each complex (Fig. 1) were constructed so as to find out the geometry with the lowest energy at the B3LYP/6-31G* level. Based on these optimized geometries, frequency calculations at the same level were carried out to verify the reasonability of optimized structures.

All quantum chemistry calculations were carried out on a Power Challenger R-10000 supercomputer with the GAUSSIAN94 program.[25] All molecular modeling was performed on an SGI workstation with the SYBYL6.2 software package.[26] Normal model analysis of the calculated vibration spectrum was carried out with the MOLDEN program.

Results and discussion

The structures of the complexes of NH_4^+ and aromatic heterocyclics

Fig. 2 depicts the optimized structures of these complexes. All the frequency calculation results of these optimized geometries showed that no imaginary frequency existed, indicating that these optimized structures were minimum energy structures. In addition, the complex structures could be divided into two types: one is a cation–π complex (Fig. 2a and 2d) and the other is the hydrogen-bonded complex formed by proton transfer from ammonium to heterocyclics (Fig. 2b and 2c). It is to our surprise that all the initial structures in Fig. 1b and Fig. 1c arrived fundamentally at the same type of complex. Some geometrical parameters are summarized in Table 1.

The structural characteristics of the cation–π complex

The optimized results showed that NH_4^+ tilts toward the plane of heterocyclics with a hydrogen atom (Table 1, Fig. 2a and 2d). It is different from the NH_4^+–C_6H_6 complex. Our previous study showed that two hydrogen atoms of NH_4^+ have an identical distance to the benzene plane in the NH_4^+–C_6H_6 complex.[10] The shortest distance between the hydrogen atom

Table 1 Some optimized geometry parameters at the B3LYP/6-31G* level (atomic numbering used is shown in Fig. 2, bond length: Å, dihedral: °)

a. NH_4^+–pyrrole (cation–π complex)

Complex		Free NH_4^+ or pyrrole	
Bond	Length	Bond	Length
R(6,1)	1.0817	R(6,1)	1.0817
R(7,2)	1.0810	R(7,2)	1.0805
R(7,6)	1.3813	R(7,6)	1.3781
R(8,3)	1.0824	R(8,3)	1.0805
R(8,6)	1.4315	R(8,6)	1.4255
R(10,4)	1.0811	R(10,4)	1.0805
R(10,8)	1.3891	R(10,8)	1.3781
R(11,5)	1.0113	R(11,5)	1.008
R(11,7)	1.3782	R(11,7)	1.3756
R(11,10)	1.3735	R(11,10)	1.3756
R(13,7)	2.7242		
R(14,8)	2.0989		
R(15,9)	1.0254	R(15,9)	1.0294
R(15,12)	1.0253	R(15,12)	1.0294
R(15,13)	1.0286	R(15,13)	1.0294
R(15,14)	1.0583	5(15,14)	1.0294
Dihedral		Dihedral	
D(10,8,6,1)	177.1954	D(10,8,6,1)	180.00
D(2,7,6,8)	176.8975	D(2,7,6,8)	180.00
D(3,8,6,7)	−175.4994	D(3,8,6,7)	180.00
D(4,10,8,6)	−175.7576	D(4,10,8,6)	180.00
D(5,11,7,6)	172.7423	D(5,11,7,6)	180.00

b. NH_4^+–imidazole (H-bonded complex)

Complex		Free NH_4^+ or imidazole	
Bond	Length	Bond	Length
R(6,1)	1.0787	R(6,1)	1.0795
R(7,2)	1.0134	R(7,2)	1.0096
R(8,3)	1.0788	R(8,3)	1.0817
R(9,4)	1.0794	R(9,4)	1.0820
R(10.12)	1.0836	R(10,12)	
R(8,6)	1.3648	R(8,6)	1.3722
R(7,6)	1.3820	R(7,6)	1.3809
R(9,7)	1.3415	R(9,7)	1.3671
R(10,9)	1.3306	R(10,9)	1.3150
R(8,10)	1.3810	R(8,10)	1.3787
R(5,12)	1.6757	R(5,12)	
R(5,10)	2.7591	R(5,10)	
R(11,5)	1.0212	R(11,5)	1.0294
R(13,5)	1.0211	R(13,5)	1.0294
R(14,5)	1.0211	R(14,5)	1.0294
Dihedral		Dihedral	
D(10,8,6,1)	180.00	D(10,8,6,1)	180.00
D(2,7,9,10)	180.00	D(2,7,6,8)	180.00
D(3,8,6,7)	179.98	D(3,8,6,7)	180.00
D(4,9,10,8)	−180.03	D(4,10,8,6)	180.00
D(6,8,10,12)	−180.05	D(5,11,7,6)	180.00
D(14,5,11,13)	112.60	D(14,5,11,13)	111.89

c. NH_4^+–pyridine (H-bonded complex)

Complex		Free NH_4^+ or pyridine	
Bond	Length	Bond	Length
R(2,1)	1.3978	R(2,1)	1.3945
R(3,2)	1.3978	R(3,2)	1.3945
R(4,3)	1.3863	R(4,3)	1.3962
R(5,4)	1.3476	R(5,4)	1.3390
R(6,1)	1.3862	R(6,1)	1.3962
R(6,5)	1.3477	R(6,5)	1.3390
R(7,1)	1.0841	R(7,1)	1.0861
R(8,2)	1.0856	R(8,2)	1.0869
R(9,3)	1.0841	R(9,3)	1.0861
R(10,4)	1.0841	R(10,4)	1.0892
R(11,6)	1.0841	R(11,6)	1.0892
R(13,5)	1.0815	R(13,5)	
R(13,12)	1.6909	R(13,12)	
R(14,12)	1.0211	R(14,12	1.0294
R(15,12)	1.0211	R(15,12)	1.0294
R(16,12)	1.0211	R(16,12)	1.0294
Dihedral		Dihedral	
D(3,2,1,7)	180.00	D(3,2,1,7)	180.00
D(5,4,3,9)	180.00	D(5,4,3,9)	180.00
D(6,5,4,10)	180.00	D(6,5,4,10)	180.00
D(13,5,4,3)	−180.00	D(13,5,4,3)	180.00
D(11,6,1,2)	180.00	D(11,6,1,2)	180.00
D(4,3,2,8)	180.00	D(4,3,2,8)	180.00

d. NH_4^+–indole (cation–π complex)

Complex		Free NH_4^+ or indole	
Bond	Length	Bond	Length
R(6,1)	1.0809	R(6,1)	1.0815
R(7,2)	1.0810	R(7,2)	1.0813
R(7,6)	1.3709	R(7,6)	1.3697
R(8,6)	1.4339	R(8,6)	1.4372
R(9,3)	1.0871	R(9,3)	1.0872
R(9,8)	1.4118	R(9,8)	1.4064
R(10,8)	1.4314	R(10,8)	1.4239
R(11,4)	1.0102	R(11,4)	1.0079
R(11,7)	1.3826	R(11,7)	1.3830
R(11,10)	1.3762	R(11,10)	1.3811
R(12,5)	1.0863	R(12,5)	1.0867
R(12,9)	1.3981	R(12,9)	1.3887
R(13,10)	1.4041	R(13,10)	1.3989
R(14,12)	1.4145	R(14,12)	1.4106
R(14,13)	1.3955	R(14,13)	1.3900
R(15,13)	1.0870	R(15,13)	1.0872
R(16,14)	1.0858	R(16,14)	1.0866
R(18,9)	2.2057	R(18,9)	
R(19,13)	2.5217	R(19,13)	
R(18,17)	1.0480	R(18,17)	1.0294
R(19,17)	1.0315	R(19,17)	1.0294
R(20,17)	1.0250	R(20,17)	1.0294
Dihedral		Dihedral	
D(11,7,6,1)	−179.51	D(11,7,6,1)	180.00
D(2,7,6,8)	178.47	D(2,7,6,8)	180.00
D(3,9,8,10)	−177.27	D(3,9,8,10)	180.00
D(4,11,7,6)	173.28	D(4,11,7,6)	180.00
D(5,12,9,8)	−177.44	D(5,12,9,8)	180.00
D(15,13,10,8)	178.08	D(15,13,10,8)	180.00
D(16,14,12,9)	−178.43	D(16,14,12,9)	180.00

of NH_4^+ and the heavy atom of pyrrole, R(14,8), is 2.10 Å, and that of indole, R(18,9), is 2.21 Å (Table 1). The perpendicular distances between the H of NH_4^+ and the heterocyclic planes are 2.05 Å (r_1, Fig. 2a) and 2.10 Å (r_2, Fig. 2d) for pyrrole and indole complexes, respectively. It seems that the perpendicular distance of NH_4^+ to the heterocyclic plane is similar and the scale of the heterocyclic ring has no significant influence on the distance. Compared with the distances of NH_4^+ to the C_6H_6 plane (2.31 Å), the distance between NH_4^+ and the heterocyclic is shorter, implying that the binding interaction in NH_4^+–heterocyclic complexes might be stronger than in the NH_4^+–C_6H_6 complex. The projection of the hydrogen atom on the heterocyclic plane (Fig. 2a and 2d) suggested that H of NH_4^+ interacts with the C=C bond rather than with the carbon or nitrogen atom.

Compared with the N–H bond length of free NH_4^+, the N–H bond lengths of NH_4^+ in these complexes were changed. The H–N bond near to the heterocyclic ring lengthened by ~0.02 Å

Table 2 CHelpG charge (Q/e) at the B3LYP/6-31G* level (atomic numbering used is shown in Fig. 2)

	NH_4^+–pyrrole		NH_4^+–imidazole		NH_4^+–pyridine		NH_4^+–indole	
Atom no.	Complex	Single	Complex	Single	Complex	Single	Complex	Single
1	0.134	0.106	0.194	0.155	−0.130	−0.371	0.190	0.154
2	0.151	0.134	0.349	0.292	0.094	0.195	0.145	0.124
3	0.114	0.106	0.194	0.066	−0.124	0.379	0.134	0.129
4	0.151	0.134	0.200	0.068	0.053	0.411	0.381	0.358
5	0.333	0.297	−0.666	−0.735	−0.061	−0.595	0.110	0.115
6	−0.158	−0.136	−0.068	−0.232	0.059	0.406	−0.388	−0.360
7	−0.071	−0.157	−0.157	−0.224	0.154	0.132	0.083	0.005
8	−0.062	−0.136	−0.097	0.152	0.120	0.053	0.182	0.227
9	0.374	0.434	0.008	0.214	0.153	0.136	−0.170	−0.256
10	−0.086	−0.157	−0.014	−0.491	0.149	0.006	0.221	0.179
11	−0.235	−0.193	0.295	0.434	0.148	0.007	−0.471	−0.447
12	0.371	0.434	0.180	0.434	−0.659	−0.735	−0.085	−0.090
13	0.272	0.434	0.292	0.434	0.169	0.434	−0.176	−0.207
14	0.163	0.434	0.290	0.434	0.293	0.434	−0.127	−0.116
15	−0.449	−0.735			0.291	0.434	0.135	0.115
16					0.291	0.434	0.123	0.096
17							−0.372	−0.735
18							0.167	0.434
19							0.220	0.434
20							0.333	0.434
21							0.367	0.434

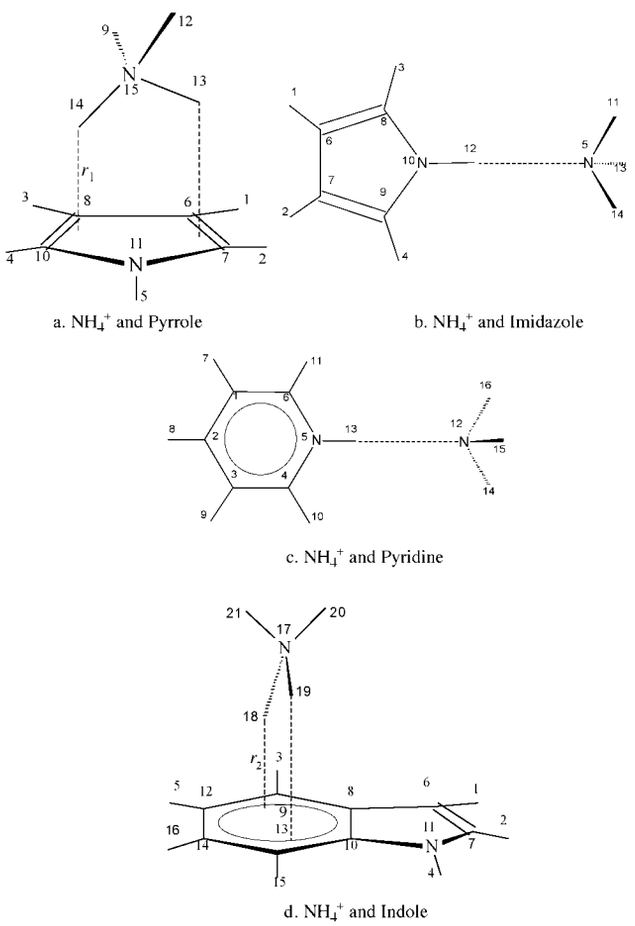

Fig. 2 Optimized structures of the complexes formed by NH_4^+ and heterocyclics at the B3LYP/6-31G* level.

and those far from the heterocyclic ring shortened slightly. The C–C bond length of heterocyclic rings near to NH_4^+ is in general lengthened by 0.01 Å. The lengthened bond lengths suggested that these bonds became weaker in complex formation.

The dihedrals in Table 1 suggested that the hydrogen atoms of the heterocyclic ring do not have the same plane with heavy atoms. As a matter of fact, these hydrogen atoms moved away from the ammonium ion. It could be due to the repulsion between cation (NH_4^+) and these hydrogen atoms, which drives them to be far apart from each other.

The structural characteristics of the hydrogen bond complex

Table 1 and Fig. 2b and 2c showed that there is a hydrogen bond between the hydrogen atom attached to the heteroatom transferred from NH_4^+ and the N atom of ammonia formed after proton transfer. Unlike the cation–π complex, the dihedrals of heterocyclic hydrogen atoms did not change significantly after the formation of the hydrogen bond complex because NH_3 interacted with the heterocyclic laterally. The hydrogen bond lengths in Fig. 2b and 2c were 1.68 and 1.69 Å, respectively, implying that the interaction between NH_3 and the protonated heterocyclic is quite strong, for these hydrogen bond lengths are quite short in comparison.

Charge population analysis

In order to investigate the charge distribution in these complexes, CHelpG charge[28] was calculated (Table 2). Regarding the cation–π complex, if it is divided into two parts, heterocyclic and ammonium, the total atomic charges of these two parts are 0.269 and 0.731 for the NH_4^+–pyrrole complex, and 0.285 and 0.715 for the NH_4^+–indole complex, respectively. The result suggested that the positive charge of NH_4^+ was partially transferred to the heterocyclic, demonstrating that electron transfer from the heterocyclic to NH_4^+ occurs when NH_4^+ binds to the heterocyclic.

In the case of the hydrogen bond complex, the total atomic charges of the formed heterocyclic cation and ammonia were 0.789 and 0.211 for the imidazolium–NH_3 complex, and 0.784 and 0.216 for the pyridinium–NH_3 complex, respectively, indicating that most of the 1 unit positive charge was transferred to heterocyclics from NH_4^+ and suggesting that proton transfer occurred while NH_4^+ bound to the heterocyclic.

The frontier orbital

The interaction mechanism of the hydrogen bond in the hydrogen bond complex is clear. Here we just tried to perform some analyses on the molecular orbital of the NH_4^+–pyrrole cation–π complex in order to investigate the interaction

Table 3 The ten largest atomic orbital coefficients of the HOMO of the NH_4^+–pyrrole complex

Atomic orbital	^6C-2p_x	^6C-3p_x	^7C-2p_x	^7C-2p_z	^7C-3p_x	^8C-2p_x	^8C-3p_x	^{10}C-2p_x	^{10}C-3p_x	^{14}H-2s
Coefficient	0.241	0.180	0.348	0.117	0.267	−0.177	−0.116	−0.339	−0.260	−0.162

Table 4 Calculated thermodynamic parameters at the B3LYP/6-31G* level (E_{inter}: Hartree; S: cal mol^{-1} K^{-1}; $E_{thermal}$, ΔE, ΔH and ΔG: kcal mol^{-1})

Initial system		E_{inter}	$E_{thermal}$	S	ΔE_{inter}	ΔH	ΔG
	Complex	−267.0948924	88.963	84.672	−22.043	−23.614	−13.787
NH_4^+–pyrrole	Pyrrole	−210.1658903	58.047	65.173			
	NH_4^+	−56.8938890	33.077	47.186			
NH_4^+– imidazole	Complex	−283.1801237	81.290	84.664	−44.999	−47.949	−36.415
	Imidazole	−226.2145545	50.573	64.545			
NH_4^+–pyridine	Complex	−305.2453132	92.882	88.186	−41.723	−41.049	−32.806
	Pyridine	−248.2849630	58.541	68.644			
NH_4^+–indole	Complex	−420.7479397	120.192	98.301	−23.455	−22.419	−14.055
	Indole	−363.8166879	85.489	79.162			

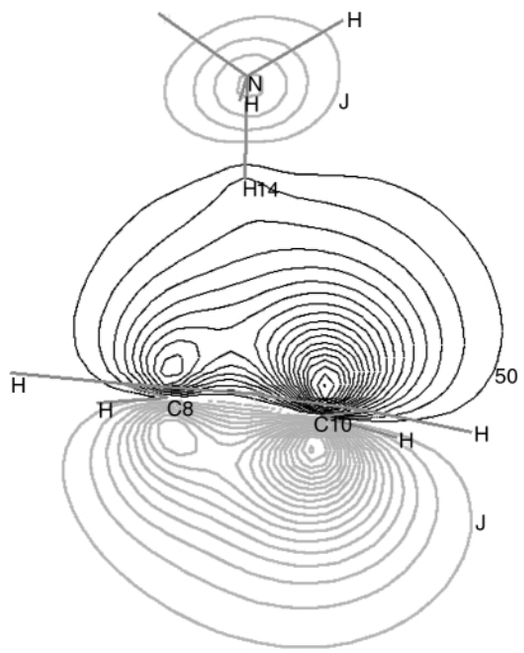

Fig. 3 The HOMO image of the NH_4^+–pyrrole complex on the plane H14–C8–C10.

mechanism between NH_4^+ and heterocyclics. We found that the HOMO (Highest Occupied Molecular Orbital) and LUMO (Lowest Unoccupied Molecular Orbital) energies were −0.20155 and 0.05095 Hartree for free pyrrole, −0.8625 and −0.21083 Hartree for free NH_4^+, −0.37674 and −0.15562 Hartree for their complexes. These energies suggested that electron transfer is possible from pyrrole to NH_4^+. Meanwhile, our analysis on all 23 occupied molecular orbitals showed that HOMO was the molecular orbital contributed by both the heterocyclic and NH_4^+. Table 3 presents the ten largest atomic orbital coefficients of HOMO. It can be seen that the HOMO is mainly composed of the s orbital of hydrogen atom H14 and the p_x orbitals of all pyrrole carbon atoms (refer to Fig. 2a). However, it is only C8 and C10 for which the atomic orbitals have the same sign as the s orbital of H14, giving the electron probability-density buildup in the region enclosed by these three nuclei. Fig. 3 depicts the HOMO image of the NH_4^+–pyrrole complex in the H14–C8–C10 plane. It is clear from Fig. 3 that H14 binds to the C8=C10 bond, suggesting that the interaction between NH_4^+ and the aromatic heterocyclic is related to s–π interaction. This conclusion is consistent with what we had deduced above based on geometrical analysis. It is different from the hydrogen bond which is related to s–p interaction, and is also different from the interaction between the transition metal ion and the aromatic ring which is related to d–π interaction.

Thermodynamic parameters

Table 4 shows the calculated results of internal energies (E_{inter}), thermal energies ($E_{thermal}$) and entropies (S) of all optimized structures at the B3LYP/6-31G* level. The thermodynamic parameters of internal energy change (ΔE_{inter}), thermal energy change ($\Delta E_{thermal}$), enthalpy change (ΔH), entropy change (ΔS) and free energy change (ΔG) for all complexes were calculated using eqns. (1)–(5) and are also listed in Table 4.

$$NH_4^+ + \text{heterocyclic} \longrightarrow \text{complex}$$

$$\Delta E_{inter} = E_{inter}(\text{complex}) - E_{inter}(NH_4^+) - E_{inter}(\text{heterocyclic}) \quad (1)$$

$$\Delta E_{thermal} = E_{thermal}(\text{complex}) - E_{thermal}(NH_4^+) - E_{thermal}(\text{heterocyclic}) \quad (2)$$

$$\Delta S = S(\text{complex}) - S(NH_4^+) - S(\text{heterocyclic}) \quad (3)$$

$$\Delta H = \Delta E_{inter} + \Delta E_{thermal} + \Delta(pv) \quad (4)$$

$$\Delta G = \Delta H - T\Delta S \quad (5)$$

Regarding the cation–π complex, the calculated ΔH was found to be −22.0 kcal mol^{-1} for the NH_4^+–pyrrole complex, and −23.5 kcal mol^{-1} for the NH_4^+–indole complex. Our previous calculation based on the B3LYP/6-31G* method showed that the ΔH of complex $NH_4^+ \cdots C_6H_6$ was −16.5 kcal mol^{-1}.[10] These results revealed that the interaction between NH_4^+ and heterocyclics is stronger than that of NH_4^+ and benzene. Furthermore, NH_4^+ interacts with C_6H_6 through two hydrogen atoms equally, the ΔH for each one is about −8.2 kcal mol^{-1}. But the interaction between NH_4^+ and the aromatic heterocyclic ring is mainly carried out through one hydrogen atom, reflecting that the interaction between H14 and the C8=C10 bond (refer to Fig. 2a) was quite strong. This is in agreement with the short interaction distance discussed above. Compared with the bond energy of F–F (F_2), 37.8 kcal mol^{-1}, strong interaction in NH_4^+–heterocyclics can also be found. The ΔH in Table 4 also showed that the binding strengths of NH_4^+ to different aromatic heterocyclics, pyrrole and indole, were similar, implying that the scale of the heterocyclic ring did not

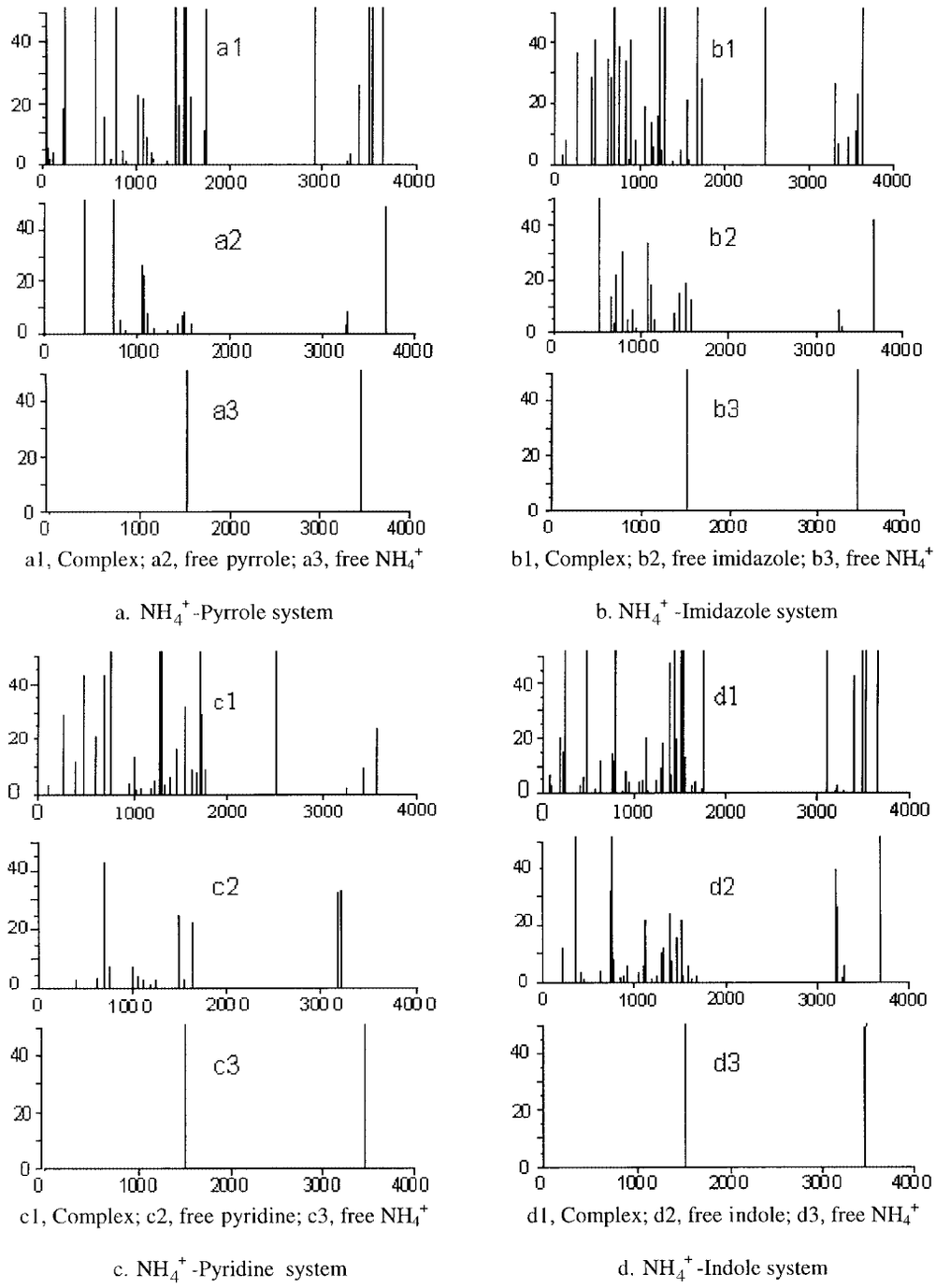

a1, Complex; a2, free pyrrole; a3, free NH_4^+

a. NH_4^+-Pyrrole system

b1, Complex; b2, free imidazole; b3, free NH_4^+

b. NH_4^+-Imidazole system

c1, Complex; c2, free pyridine; c3, free NH_4^+

c. NH_4^+-Pyridine system

d1, Complex; d2, free indole; d3, free NH_4^+

d. NH_4^+-Indole system

Fig. 4 Theoretical IR spectra at the B3LYP/6-31G* level.

affect the binding strength significantly. We also noticed that the predicted binding energy between indole and NH_4^+ at the 6-31G*//3-21G-MP2 level reported by Basch and Stevens is 25.9 kcal mol^{-1}.[3] However, our previous calculated results showed that different basis sets used in structural optimization and energy calculation resulted in significant error.[10] Hence, we thought that our calculated ΔH, −23.5 kcal mol^{-1}, for the NH_4^+–indole complex was more reliable.

Regarding the hydrogen bond complex, the ΔH for imidazolium–NH_3 and pyridinium–NH_3 complexes were −47.9 and −41.0 kcal mol^{-1}, respectively. They are larger than the ΔH of the cation–π complex, reflecting that the formation of such complexes should be favorable to the stability of the whole system. In order to reveal the strength of the hydrogen bond in this type of complex, we performed a calculation on free NH_3 and imidazolium at the B3LYP/6-31G* level. The E_{inter}, $E_{thermal}$ and S of NH_3 were −56.5479469 Hartree, 23.479 kcal mol^{-1} and 48.157 cal mol^{-1} K^{-1}, respectively; those of imidazolium were −226.5921736 Hartree, 55.977 kcal mol^{-1} and 63.384 cal mol^{-1} K^{-1}, respectively. Therefore, the ΔH of the complex NH_3–imidazolium formed by NH_3 and imidazolium was −23.9 kcal mol^{-1} and ΔG was −15.9 kcal mol^{-1}, suggesting that the hydrogen bond in the protonated heterocyclic–NH_3 complex is very strong. Accordingly, the contribution of proton transfer to the whole ΔH is [−47.9 − (−23.9)] = −24.0 kcal mol^{-1}. Imidazole or pyridine has a nitrogen atom with localized lone-pair electrons that has the ability to accept a proton. However, the heteroatoms in pyrrole and indole have no strong ability to accept a proton for their lone-pair electrons are delocalized. Hence, we could deduce that if the heteroatom has localized lone-pair electrons, the hydrogen bond complex is the favorable product. If the heteroatom has no localized lone-pair electrons, the cation–π complex should be the final product.

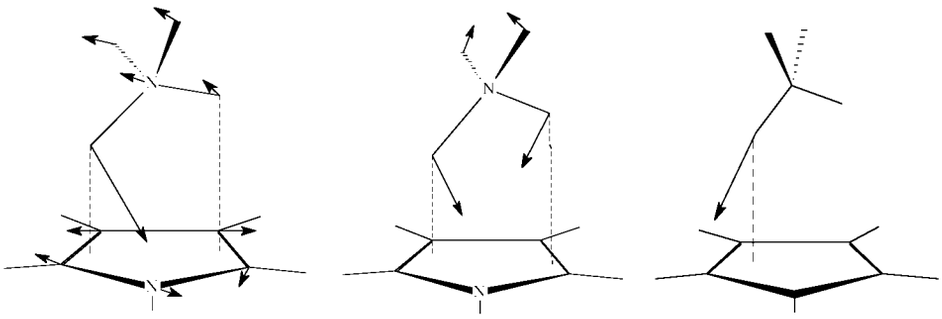

a. Complex formed by NH_4^+ and pyrrole

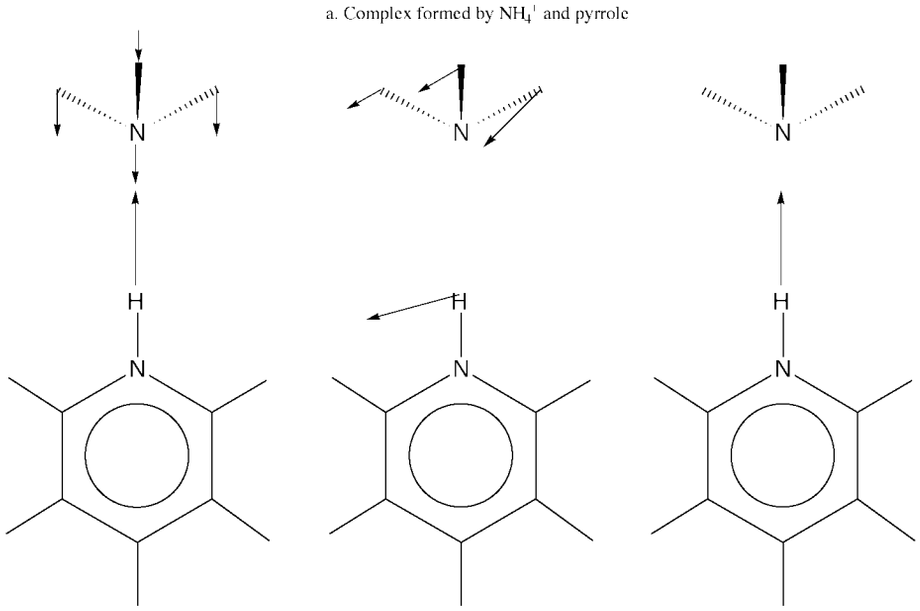

b. Complex formed by NH_4^- and pyridine

Fig. 5 Normal mode analysis results.

In order to investigate other possible conformations of the hydrogen bond complex, geometrical optimization of different initial structures constructed by NH_3 and the protonated heterocyclic, with NH_3 above the heterocyclic plane, was carried out at the B3LYP/6-31G* level. The optimization result did not show that the cation–π complex was a stable conformation, implying that the strong tendency between the NH_3 and protonated heterocyclic is to form the hydrogen bond complex as shown in Fig. 2b and 2c. However, our calculated results also showed that the N of NH_3 can possibly interact with other hydrogen atoms besides the hydrogen atom attached to the heteroatom of the heterocyclic (refer to Fig. 2b and 2c), but the binding strength is weaker than the interaction between the N of NH_3 and the heteroatom hydrogen. For example, if the interaction is located at N12 and H8 rather than H13 in Fig. 2c, the ΔH is -10.36 kcal mol^{-1}. These calculated results showed that once the protonated heterocyclic is formed, all its hydrogen atoms are possible hydrogen bond donors, implying that the role of the protonated heterocyclic structure in biology is fairly complicated and important.

Experimental and theoretical studies of the cation–π interaction had shown that the cation could be pulled into a hydrophobic binding site of a receptor.[27] In addition, based on our calculated results, the final product could be different. The hydrogen bond complex might be formed besides the cation–π complex by proton transfer from NH_4^+ to the heteroatom.

Normal mode analysis of calculated IR

The IR spectra of free NH_4^+, heterocyclics and their complexes at the B3LYP/6-31G* level are depicted in Fig. 4.

Regarding cation–π complexes (Fig. 4a and 4d), when compared with free NH_4^+ and heterocyclics, the complexes have three groups of new bands, which should be the intrinsic bands of these complexes. The first group consists of bands below ~250 cm^{-1}. Normal mode analysis on these bands revealed that they correspond to the rocking of NH_4^+ above the heterocyclic plane. The second group is made up of the bands located at ~1750 cm^{-1}. Normal mode analysis showed that these bands belong to the bending of H–N–H of NH_4^+. The third group consists of bands at ~3000 cm^{-1}, which relate to the stretching of the H–N bond of NH_4^+ toward the π face of the heterocyclic plane. All these vibrations resulted in a change of the distance between NH_4^+ and the heterocyclics. As an example, Fig. 5a depicts the normal mode analysis results for the NH_4^+–pyrrole complex.

In the case of hydrogen bond complexes, there were also three groups of new bands. The first group is under ~300 cm^{-1}. Normal mode analysis showed that these vibration modes are related to the relative movement of NH_3 against the heterocyclic. The second group is located at ~1700 cm^{-1}, corresponding to the rocking of the hydrogen-bonded hydrogen atom on the plane of the heterocyclic ring. The third group consists of bands at about 2500 cm^{-1}, belonging to N–H bond stretching

of the heterocyclic. All these vibrations also bring about a change of hydrogen bond length. Fig. 5b depicts the normal mode analysis results for the NH_4^+–pyridine complex.

Conclusion

From the results discussed above, we concluded that NH_4^+ binds to aromatic nitrogen heterocyclics more strongly than to benzene. However, the binding interaction results in two types of complexes. One is the NH_4^+–heterocyclic cation–π complex, and the other is the hydrogen bond complex. If the heteroatom has no localized lone-pair electrons, the NH_4^+–heterocyclic cation–π complex will be formed with NH_4^+ above the heterocyclic plane. If the heteroatom has localized lone-pair electrons, then proton transfer is carried out from NH_4^+ to the heterocyclic and the final product is the hydrogen bond complex.

In the case of the cation–π complex, although the binding interactions in both NH_4^+–heterocyclic and NH_4^+–C_6H_6 complexes are related to s–π interaction, the interaction between NH_4^+ and the heterocyclic is stronger than that of NH_4^+ and benzene. We have also shown that whilst NH_4^+ binds to the π bond of the heterocyclic mainly through one hydrogen atom, it binds to benzene equally through two hydrogen atoms. Our calculated results showed that the interaction intensities between NH_4^+ and pyrrole or indole are similar, and ring scale has no significant influence on the intensity. Regarding the hydrogen bond complex, the enthalpy change for the whole process is larger than the formation of the cation–π complex. The strongest hydrogen bond interaction is located at the H atom attached to the heteroatom and ammonia, but the calculated results also showed that all the hydrogen atoms of the protonated heterocyclic are likely to be used as hydrogen bond donor.

The calculated IR spectra showed that three new groups appear after the formation of either the cation–π or the hydrogen bond complex. Normal mode analysis showed that all these new bands were related to the relative motion of NH_4^+/NH_3 and heterocyclics.

We conclude by highlighting that the NH_4^+–heterocycle system is a better model than the NH_4^+–C_6H_6 model to study the interaction mechanism between cations and aromatic nitrogen heterocyclic structures in biology. Although the NH_4^+–C_6H_6 model can be used to describe the nature of the interaction between NH_4^+ and the π system, the NH_4^+–heterocycle model can be used to illustrate both the nature and the complexity of the interaction between the ammonium group and aromatic amino acid residues of proteins or the aromatic bases of nucleic acids.

Acknowledgements

This research was partially supported by the National Natural Science Foundation of China (Grant 29725203) and the "863" High Technology Program of China (Grant 863-103-04-01). Thanks are given to Professor Jian-De Gu, Dr Jian-Zong Chen and Mr Mao-Wei Lin for fruitful discussions and help. Quantum chemistry calculations were performed at The Network Information Center, Chinese Academy of Sciences.

References

1 J. C. Ma and D. A. Dougherty, *Chem. Rev.*, 1997, **97**(5), 1303.
2 C. A. Deakyne and M. Meot-Ner, *J. Am. Chem. Soc.*, 1985, **107**, 474.
3 H. Basch and W. J. Stevens, *J. Mol. Struct.* (*THEOCHEM*), 1995, **338**, 303.
4 S. K. Burley and G. A. Petsko, *FEBS Lett.*, 1986, **203**, 139.
5 O. Mó, M. Yáñez and J. Elguero, *J. Org. Chem.*, 1987, **52**, 1713.
6 M. A. Petti, T. J. Shepodd, J. R. E. Barrans and D. A. Dougherty, *J. Am. Chem. Soc.*, 1988, **110**, 6825.
7 P. Mátyus, K. Fuji and K. Tanaka, *Tetrahedron*, 1994, **50**(8), 1405.
8 W. L. Zhu, H. L. Jiang, J. Z. Chen, J. D. Gu, K. X. Chen, Y. Cao and R. Y. Ji, *Sci. China Ser. B: Chem.*, 1998, **41**(6), 616.
9 X. J. Tan, H. L. Jiang, W. L. Zhu, K. X. Chen and R. Y. Ji, *J. Chem. Soc.*, *Perkin Trans. 2*, 1999, 107.
10 H. L. Jiang, W. L. Zhu, X. J. Tan, J. D. Gu, J. Z. Chen, M. W. Lin, K. X. Chen and R. Y. Ji, *Sci. China Ser. B: Chem.*, 1998, **41**(5), 535.
11 K. Murayama and K. Aoki, *Chem Commun.*, 1997, 119.
12 Y. J. Zhang and K. M. Merz, Jr, *J. Comput. Chem.*, 1992, **13**(9), 1151.
13 S. Mecozzi, A. P. West, Jr and D. A. Dougherty, *J. Am. Chem. Soc.*, 1996, **118**, 2307.
14 J. W. Caldwell and P. A. Kollman, *J. Am. Chem. Soc.*, 1995, **117**, 4177.
15 J. Y. Lee, S. J. Lee, H. S. Choi, K. S. Kim and T. K. Ha, *Chem. Phys. Lett.*, 1995, **232**, 67.
16 D. Becke, *J. Chem. Phys.*, 1993, **98**, 5648.
17 S. Mecozzi, A. P. West, Jr and D. A. Dougherty, *Proc. Natl. Acad. Sci.*, 1996, **93**, 10566.
18 J. D. Gu, K. X. Chen, H. L. Jiang, W. L. Zhu, J. Z. Chen and R. Y. Ji, *Chem. Phys. Lett.*, 1997, **277**(1–3), 234.
19 W. L. Zhu, H. L. Jiang, J. D. Gu, J. Z. Chen, J. K. Shen, K. X. Chen and R. Y. Ji, *J. Mol. Struct.* (*THEOCHEM*), 1999, in the press.
20 W. L. Zhu, H. L. Jiang, X. J. Tan, J. Z. Chen, Y. F. Zhai, J. D. Gu, M. W. Lin, K. X. Chen, R. Y. Ji and Y. Cao, *Acta Chim. Sin.*, 1999, **57**, 852.
21 H. L. Jiang, W. L. Zhu, X. J. Tan, J. Z. Chen, Y. F. Zhai, D. X. Liu, L. Zhao, K. X. Chen and R. Y. Ji, *Acta Chim. Sin.*, 1999, **57**, 860.
22 A. M. de Vos, M. Ultsch and A. A. Kossiakoff, *Science*, 1992, **255**, 306.
23 J. L. Sussman, M. Harel, F. Frolow, C. Oefner, A. Goldman, L. Toker and I. Silman, *Science*, 1991, **253**, 872.
24 X. Cheng, S. Kumar, J. Posfai, J. W. Pflugrath and R. J. Roberts, *Cell*, 1993, **74**, 299.
25 GAUSSIAN94, *Gaussian*, *Inc.*, Pittsburgh, PA, 1995.
26 SYBYL6.2, *Tripoes Associates*, St. Louis (MO), 1995.
27 D. A. Dougherty and D. A. Stauuffer, *Science*, 1990, **250**, 1558.
28 C. M. Breneman and K. B. Wiberg, *J. Comput. Chem.*, 1990, **11**, 361.

Paper 9/02663K